

Dalton Transactions

Accepted Manuscript



This is an *Accepted Manuscript*, which has been through the Royal Society of Chemistry peer review process and has been accepted for publication.

Accepted Manuscripts are published online shortly after acceptance, before technical editing, formatting and proof reading. Using this free service, authors can make their results available to the community, in citable form, before we publish the edited article. We will replace this *Accepted Manuscript* with the edited and formatted *Advance Article* as soon as it is available.

You can find more information about *Accepted Manuscripts* in the [Information for Authors](#).

Please note that technical editing may introduce minor changes to the text and/or graphics, which may alter content. The journal's standard [Terms & Conditions](#) and the [Ethical guidelines](#) still apply. In no event shall the Royal Society of Chemistry be held responsible for any errors or omissions in this *Accepted Manuscript* or any consequences arising from the use of any information it contains.

BaCu₂Se₂ based compounds as promising thermoelectric materials

Jing Li,^{ab} Li-Dong Zhao,^c Jiehe Sui,^{*a} David Berardan,^{*b} Wei Cai,^a and Nita Dragoeb^b

^aSchool of Materials Science and Engineering, Harbin Institute of Technology, Harbin 150001, China. E-mail: suijiehe@hit.edu.cn

^bSP2M, ICMO (CNRS UMR 8182), Univ. Paris Sud, Orsay F91405, France.

E-mail: david.berardan@u-psud.fr

^cSchool of Materials Science and Engineering, Beihang University, Beijing 100191, China

Jing Li and Li-Dong Zhao contributed equally to this work.

KEYWORDS BaCu₂Se₂; thermoelectric; doping; carrier concentration; low thermal conductivity

ABSTRACT: In the past few years, many studies have been devoted to the thermoelectric properties of copper selenides and sulfides, and several families of materials have been developed with promising performances. In this paper, we report on the synthesis and thermoelectric properties of Na-doped BaCu₂Se₂ from 20K to 773 K. By Na doping at Ba site, the electric conductivity can be increased by 2 orders of magnitude, and the power factor can reach 8.2 $\mu\text{Wcm}^{-1}\text{K}^{-2}$ at 773K. Combined with a low thermal conductivity of 0.65 $\text{Wm}^{-1}\text{K}^{-1}$, ZT of 1.0 has been obtained for Ba_{0.925}Na_{0.075}Cu₂Se₂ at 773 K, which is the highest value reported in this family by now. However, the BaCu₂Se₂ volatilizes from 473K, so protecting coating is necessary for its application. Besides, we studied thermal expansion coefficient of BaCu₂Se₂ in this paper.

Introduction

Thermoelectric materials are currently receiving a significant scientific attention since they are capable of converting waste heat into electrical power. The power generation efficiency of a thermoelectric device is determined by the dimensionless figure of merit ZT, $ZT = (S^2\sigma/\kappa)T$, where S, σ , κ and T are the Seebeck coefficient, the electrical conductivity, the thermal conductivity, and the absolute temperature, respectively. Several approaches to enhance ZT have emerged in the last decades,

most of these approaches aim to gain a high power factor ($S^2\sigma$) while obtaining a low lattice thermal conductivity (κ). Alternatively, one can also seek high thermoelectric performance in pristine materials with intrinsically low thermal conductivity. Copper-containing chalcogenides have been in the limelight of solid state research due to their large variety of crystal structures¹⁻⁴ and potential for widespread applications, including magnetic semiconductor,⁵ high-Tc superconductors,⁶ or transparent conductor⁷. Recently, copper chalcogenides based materials have attracted extensive interest in the thermoelectric community due to low thermal conductivities, which lead to the promising excellent thermoelectric properties: BiCuSeO⁸ ($\kappa\sim 0.6 \text{ Wm}^{-1}\text{K}^{-1}$, $ZT\sim 1.4$ for textured Ba-doped sample at 923K), Cu₂CdSnSe₄ ($\kappa\sim 0.8 \text{ Wm}^{-1}\text{K}^{-1}$, $ZT\sim 0.65$ at 773K)⁹, Cu₂ZnGeSe₄¹⁰ ($\kappa\sim 0.8 \text{ Wm}^{-1}\text{K}^{-1}$, $ZT\sim 0.45$ at 670K), Cu₂ZnSnSe¹¹ ($\kappa\sim 0.8 \text{ Wm}^{-1}\text{K}^{-1}$, $ZT\sim 0.91$ at 860 K), Cu₃Sb_{1-x}Sn_xSe₄¹² ($\kappa\sim 1.0 \text{ Wm}^{-1}\text{K}^{-1}$, $ZT\sim 1.05$), Cu₂SnSe₃¹³ ($\kappa\sim 0.74 \text{ Wm}^{-1}\text{K}^{-1}$, $ZT\sim 0.33$ at 650K), CuAgSe^{14a, b)} ($\kappa\sim 0.47 \text{ Wm}^{-1}\text{K}^{-1}$, $ZT\sim 0.95$ at 623 K), CuAgS^{14c)} ($\kappa\sim 0.52 \text{ Wm}^{-1}\text{K}^{-1}$ at 550 K), Cu₂Se^{15a)} ($\kappa\sim 1 \text{ Wm}^{-1}\text{K}^{-1}$, $ZT\sim 1.5$ at 1000K), Cu₂S^{15b)} ($0.6 \text{ Wm}^{-1}\text{K}^{-1}$, $ZT\sim 1.7$ at 1000K), Cu₁₂Sb₄S₁₃¹⁶⁾ ($\kappa\sim 1.5 \text{ Wm}^{-1}\text{K}^{-1}$, ZT above 0.8 at 700K), CuInTe₂¹⁷⁾ ($\kappa\sim 1 \text{ Wm}^{-1}\text{K}^{-1}$, $ZT\sim 1.18$ at 850K), and CuGaTe₂¹⁸⁾ ($\kappa\sim 1.35\times 10^{-3} \text{ Wm}^{-1}\text{K}^{-1}$, $ZT\sim 1.4$ at 950K).

Herein, we report our results on another copper chalcogenide, BaCu₂Se₂ system. The crystal structure and transport properties of BaCu₂Ch₂ (Ch=S, Se and Te) have been studied by few groups to date.¹⁹⁻²⁶ For Ch = S and Se, two structure-types can be stabilized: the orthorhombic BaCu₂S₂-type and tetragonal ThCr₂Si₂-type.²⁰⁻²³ Only the BaCu₂S₂ structure has been reported for BaCu₂Te₂²⁰⁻²³. The electrical conductivity of β -BaCu₂S₂ and α -BaCu₂Se₂ is moderate, 49 Scm^{-1} ²⁰, 5.5 Scm^{-1} ²¹, respectively, and 125 Scm^{-1} for BaCu₂Te₂²¹. The electric conductivity can be improved by 1 order of magnitude by K doping in β -BaCu₂S₂, but the influence of doping on the electrical properties of BaCu₂Se₂ has not been studied to date experimentally. All the three compounds exhibit high Seebeck coefficient S ($216 \mu\text{VK}^{-1}$, $390\mu\text{VK}^{-1}$ and $127\mu\text{VK}^{-1}$) and low thermal conductivity κ , $0.86 \text{ Wm}^{-1}\text{K}^{-1}$ ²⁰, $1.5 \text{ Wm}^{-1}\text{K}^{-1}$, and $2 \text{ Wm}^{-1}\text{K}^{-1}$ ²¹ for Ch= S, Se and Te respectively at room temperature (it is noteworthy that these later values were overestimated due to radiation losses during the measurement as they were measured in steady-state conditions, contrary to the former one that was measured using a Laser Flash method), which make them promising thermoelectric materials. Indeed, thermoelectric figure of merit ZT of 0.28 at 820K has been reported for K doped β -BaCu₂S₂. However, no investigation has

been reported up to now regarding the thermoelectric property of doped BaCu_2Se_2 above room temperature.

In this work, we choose Na as an acceptor dopant at Ba site, to optimize the carrier concentration and enhance the power factor of BaCu_2Se_2 . Results show that the electric conductivity can be increased by 2 orders, and the power factor of $8.2 \mu\text{Wcm}^{-1}\text{K}^{-2}$ at 773K was realized. Combined with a low thermal conductivity of $0.65 \text{Wm}^{-1}\text{K}^{-1}$, ZT of 1.0 has been obtained for $\text{Ba}_{0.925}\text{Na}_{0.075}\text{Cu}_2\text{Se}_2$ at 773 K. The thermal stability and phase stability were studied up to 873 K.

Experimental details

The $\text{Ba}_{1-x}\text{Na}_x\text{Cu}_2\text{Se}_2$ ($x=0, 0.005, 0.01, 0.015, 0.02, 0.025, 0.05, 0.075$ and 0.1) powders were prepared by a two-step solid-state route. In the first step, the BaSe precursor was synthesized by heating Ba bulk and Se powder in sealed evacuated silica tubes coated with carbon at 873K for 24h. The Na_2Se precursor was previously synthesized by heating Na bulk and Se powder in sealed silica tubes coated with carbon at 1173K for 5h. The obtained BaSe and Na_2Se powders were single phase as confirmed by X-ray diffraction measurements. Then the BaSe, Cu, Se and Na_2Se as starting materials were mixed in stoichiometric amount as given by the formula $\text{Ba}_{1-x}\text{Na}_x\text{Cu}_2\text{Se}_2$. The thoroughly mixed powders were pressed into pellets and sealed in evacuated silica tubes coated with carbon, followed by heating at 958K for 48 h. The obtained bulks were ground into powders and then densified by spark plasma sintering (SPS-511S) at 723K during 10min using graphite molds and dies with a pressure of 100 MPa under argon to form disk-shaped samples of $\text{Ø} 10$ mm and 3 mm in thickness. The resulting density of the SPS processed samples was 94% of the theoretical density.

Room temperature X-ray diffraction (XRD) characterization was performed using a Panalytical X'Pert diffractometer by using a $\text{Cu-K}\alpha 1$ radiation, with a Ge (111) incident monochromator and a X'celerator detector. High temperature XRD patterns were recorded using a Bruker D8 Advance diffractometer with an Anton Paar TTK chamber. Rietveld refinement was performed using FULLPROF software. Seebeck coefficient (S) and electrical resistivity (ρ) were measured on bars cut from the pellets, with typical size $10 \times 2 \times 2 \text{mm}^3$. The S and ρ measurements from 20 to 300 K were performed simultaneously by the differential method with two T-type thermocouples by using the slope of $\Delta V-\Delta T$ curve with gradients up to about 0.2

K/mm, by using a laboratory made system in a He-free cryostat. S and ρ from room temperature to 773 K were measured by Ulvac Riko ZEM-3 instrument (ZEM-3, ULVAC-RIKO, Japan) under a helium atmosphere. Hall effect measurements were performed in a Quantum Design Physical Properties Measurement System (PPMS) environment using a Keithley 2400 current source and a Keithley 2182A nanovoltmeter, under magnetic fields from -9T to 9T. The thermal diffusivity (D) was measured in a disk-shaped sample of $\text{\O}10\text{mm}$ and 1–2 mm in thickness by using a laser flash diffusivity method (NETZSCH, LFA457, Germany). The thermal conductivity (κ) was calculated by the equation $\kappa = DC_p d$. C_p from 300K to 400 K was measured using a Quantum Design physical properties measurement system (PPMS); C_p above 400K was estimated from linear extension of values as measured from 300K to 400 K. The density d was measured using the dimensions and weight.

Room temperature optical diffuse reflectance measurements were performed on finely ground powders to probe optical energy gap of the series. The spectra were collected in the Varian Cary 5000 double-beam, double-monochromator spectrophotometer (Ultraviolet-Visible absorption Spectra). Scanning electron microscopy (SEM) studies were performed using a Hitachi S-3400N VP-SEM equipped with an Oxford detector for energy dispersive X-ray spectroscopy (EDS). The samples used for SEM were polished using a suspension of 50 nm Al_2O_3 particles. Thermogravimetric analysis was performed using a Setaram Setsys Evo under an Ar atmosphere in the temperature range from room temperature to 873 K with a rate of 5 K min^{-1} .

Results and discussion

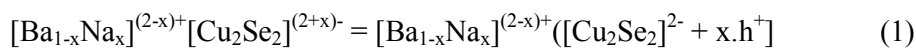
Fig. 1a) shows the observed XRD pattern and Rietveld refinement of undoped BaCu_2Se_2 , which crystallizes in the BaCu_2S_2 -type structure. The simulated pattern by the Rietveld method agrees very well with the measured XRD pattern as shown in the difference profile. The orthorhombic structure, drawn in Fig. 1b), consists of a three dimensional Cu–Se network with Ba atoms residing in channels along the b-axis. The CuSe_4 tetrahedra are connected by sharing both vertices and edges. The Cu atoms construct zigzag chains of CuSe_4 tetrahedra.

Fig. 2a) shows powder XRD patterns of all the Na doped BaCu_2Se_2 samples. All the peaks can be indexed by BaCu_2Se_2 characteristic peaks (PDF#79-1647), no second phase can be observed. The cell parameters for the undoped sample are $a =$

9.575 Å, $b = 4.202$ Å and $c = 10.755$ Å. Fig. 2b) shows the lattice parameter variations as a function of Na doping fractions. The radii of Na^+ (0.97Å) is much smaller than that of Ba^{2+} (1.34Å), however, only faint lattice parameter change can be observed with increasing Na doping fraction, which is probably related to the fact that the Ba atoms are located along the channels, the substitution of Ba with Na does not affect significantly the Cu-Se rigid network. This result is in good agreement with the previous report on K doped $\beta\text{-BaCu}_2\text{S}_2$.²⁰ The band gap of BaCu_2Se_2 is about 1.8 eV, as shown in Fig. 2c), consistent with the value determined by McGuire et al.²¹ Indeed, the electronic band structure close to the top of the valence band originates mainly from Se-p and Cu-d states and is not influenced by the Na doping.

The scanning electron microscopy image and element mapping of $\text{Ba}_{0.9}\text{Na}_{0.1}\text{Cu}_2\text{Se}_2$ are shown in Fig. 3. The uniform distributions of Ba, Cu, Se and Na for the $\text{Ba}_{0.9}\text{Na}_{0.1}\text{Cu}_2\text{Se}_2$ samples suggest that the synthesized material is homogenous.

Assuming a simple electrons counting, the substitution of one Ba^{2+} atom by one Na^+ atom in BaCu_2Se_2 should lead to one hole transfer, as:



The former value is much higher than the one that could be expected from a large band gap semiconductor. This difference most probably originates from the presence of a faint concentration of copper vacancies, similarly to the behavior observed in the BiCuSeO family⁸.

As shown in Fig. 4a), the carriers concentration indeed increases from $1.7 \times 10^{18} \text{ cm}^{-3}$ for the undoped sample to $2.6 \times 10^{20} \text{ cm}^{-3}$ for the $\text{Ba}_{0.9}\text{Na}_{0.1}\text{Cu}_2\text{Se}_2$. Indeed, a copper vacancies concentration as low as 7.4×10^{-4} per unit cell would be sufficient to induce such a carriers concentration. Taken together, the elements distributions and the increase of carriers concentration with doping level indicate the Na was successfully introduced into the BaCu_2Se_2 lattice. The measured carriers concentration is lower than the nominal one (e.g. measured $2.6 \times 10^{20} \text{ cm}^{-3}$ vs. nominal $9.2 \times 10^{20} \text{ cm}^{-3}$ for $\text{Ba}_{0.925}\text{Na}_{0.075}\text{Cu}_2\text{Se}_2$), estimated by taking into account the unit cell volume and the nominal Na concentration and assuming one free hole per Na atom. This difference could possibly be explained by Na loss during the synthesis. However, it could also be an indication of a poor doping efficiency of Na due to its much smaller ionic size as compared to Ba, which would lead to poor charge transfer to the Cu-Se network. Thus, it would be interesting to compare the doping efficiency of Na^+ and K^+ in BaCu_2Se_2 , the ionic radius of K^+ being very close to that of Ba^{2+} .

As the substitution of Ba^{2+} by Na^+ hardly affects the Cu-Se conducting network, the holes' mobility is almost constant in the whole series, of the order of $\mu = 10\text{-}15 \text{ cm}^2\text{V}^{-1}\text{s}^{-1}$ at room temperature, consistent with the value reported by McGuire et al.²¹ in the undoped compound. The Fig. 4b) shows the typical temperature behavior of the holes mobility (here for $\text{Na}=0.02$), with a decreasing trend characteristic of degenerate semiconductors.

Fig. 5 shows the temperature dependences of electrical conductivity, Seebeck coefficient, and power factor for $\text{Ba}_{1-x}\text{Na}_x\text{Cu}_2\text{Se}_2$ samples from 20 K to 773 K. The electrical conductivity of the undoped BaCu_2Se_2 is 3.1 Scm^{-1} at 300 K, consistent with the value obtained by McGuire et al.²¹ In the entire temperature measurement range, Fig. 5a) and b), the electrical conductivity increases with increasing Na content, reaches a maximum of 420 Scm^{-1} at room temperature for $\text{Ba}_{0.925}\text{Na}_{0.075}\text{Cu}_2\text{Se}_2$, and it seems to get saturated when $x=0.1$. For samples with $x \leq 0.015$, the increasing electrical conductivity with temperature indicates a semiconductor-like behavior, and change to a metallic-like behavior as $x > 0.015$. The sharp improvement of electrical conductivity with Na doping contents is consistent with the increased carrier concentration.

All samples show positive S values indicating p-type semiconducting behavior, Fig. 5c) and d), which is consistent with the positive Hall coefficient. At 20K, S of the undoped BaCu_2Se_2 is $20 \text{ }\mu\text{VK}^{-1}$, it increases with rising temperature and reaches a value of $349 \text{ }\mu\text{VK}^{-1}$ at 300 K. The Seebeck coefficient decreases with increasing Na content to $73 \text{ }\mu\text{VK}^{-1}$ for $\text{Ba}_{0.90}\text{Na}_{0.10}\text{Cu}_2\text{Se}_2$ sample at room temperature.

The temperature dependent power factor generally increases linearly with increasing temperature (Fig. 5e and f). The Na doped BaCu_2Se_2 samples show an enhanced power factor as compared to the undoped sample because of their strongly improved electrical conductivity. The highest power factor of $8.2 \text{ }\mu\text{Wcm}^{-1}\text{K}^{-2}$ is obtained at 773 K when $x= 0.075$. The uncertainty of the Seebeck coefficient and electrical conductivity measurements is 5% for instruments below and above 300K. Along with temperature discrepancy, the difference between end value of low temperature range and starting value of high temperature range is within error bar of the instruments.

Fig. 6a) shows the specific heat capacity of BaCu_2Se_2 , the room temperature value measured by PPMS is consistent with the Dulong-Petit law. The specific heat capacity increases with temperature, and is slightly larger than Dulong-Petit. Thus, C_p

of all the samples above 400K was estimated from linear extension of the as measured values from 300 to 400K in order to get an upper limit. Therefore, the thermal conductivity presented here is probably slightly overestimated and constitutes an upper limit. Fig. 6 b) shows the thermal diffusivity as a function of temperature for BaCu₂Se₂ samples. At room temperature, the total thermal conductivity of the BaCu₂Se₂ sample is $\kappa_{\text{tot}}=0.68 \text{ Wm}^{-1}\text{K}^{-1}$ as shown in Fig. 6 c), which is approximately 50% lower than the value of around $1.5 \text{ Wm}^{-1}\text{K}^{-1}$ obtained using a steady-state method which was probably overestimated due to the radiative heat losses, as underlined by McGuire et al.²¹ The total thermal conductivity increases with increasing Na content is due to the enhanced electrical thermal conductivity. For all samples, the total thermal conductivity decreases with increasing temperature, as expected for crystalline compounds with umklapp phonons scattering.

The lattice thermal conductivity, κ_{lat} , was estimated by subtracting the electronic part, κ_{ele} , from the κ_{tot} according to the Wiedemann-Franz law. The Lorenz number L can be estimated by fitting of the respective Seebeck coefficient to estimate the reduced chemical potential (η). The lattice thermal conductivity is dominant for all samples, and roughly obeys a T^{-1} relation (inset in Fig. 6e), which can be attributed to umklapp-processes being predominant at elevated temperatures. As shown in Fig. 6e), the lattice thermal conductivity slightly decreases with increasing Na content because of point defects scattering caused by the size and the atom mass difference between Na and Ba. The lattice thermal conductivity of BaCu₂Se₂ is much lower than the observed $1.5 \text{ Wm}^{-1}\text{K}^{-1}$ at room temperature^{27,28} in Phonon Glass Electron Crystal (PGEC) materials like skutterudites and clathrates and is of same order of BiCuSeO⁸. Beside the large average atomic mass of BaCu₂Se₂ (84.47g/mol atom) and its quite complex and large unit cell, which are generally associated with low thermal conductivity²⁹⁻³², the peculiar crystal structure could also play a role. The phonons propagation in this family of materials should be mostly driven by the Cu-Se framework. Ba atoms lie in the middle of 1D channels inside this framework and could lead to low energy modes which would reduce heat propagation. It is believed that the lattice dynamic studies would be of fundamental interest in order to understand the original reasons of low thermal conductivity.

The power factor values obtained in Na-doped BaCu₂Se₂ are lower than the ones observed in state-of-the-art thermoelectric materials: PbTe (PF~25 $\mu\text{Wcm}^{-1}\text{K}^{-2}$, ZT~1.6-2.0)³³⁻³⁵, PbSe (PF~14 $\mu\text{Wcm}^{-1}\text{K}^{-2}$, ZT~1.2)³⁶, Bi₂Te₃ (PF~30 $\mu\text{Wcm}^{-1}\text{K}^{-2}$,

ZT~1.1-1.75)^{37,38}. However, the low thermal conductivity contributes to a high ZT of 1.0 at 773K for Ba_{0.925}Na_{0.075}Cu₂Se₂, Fig. 6f), which is probably underestimated (due to Cp estimation). This value is promising in a new compound, and ZT could be further enhanced through carriers concentration optimization.

To highlight the potential application of BaCu₂Se₂, the properties of thermal expansion and thermal stability are also as same important as a figure of merit. Fig. 7a) shows the XRD patterns of BaCu₂Se₂ recorded from room temperature to 873K under argon atmosphere. No new structure can be observed up to 773K, and only a shift of the Bragg peaks can be noticed originating from lattice expansion. However, a few impurity peaks occur above 823K (easily observed around 2θ=25°), indicating a decomposition of the BaCu₂Se₂ phase. Fig. 7b) shows the temperature dependence of the lattice parameters, obtained from Rietveld refinement of the XRD patterns. a, b and c continuously increase with increasing temperature. As it could be expected from the crystal structure, the thermal expansion coefficient is slightly anisotropic as estimated from the temperature dependence of the lattice parameters, with a larger value in the b direction, and it decreases with increasing temperature, from 30×10⁻⁶ K⁻¹ at room temperature to 20×10⁻⁶ K⁻¹ at 873K for a and c, and from 37×10⁻⁶ K⁻¹ at room temperature to 32×10⁻⁶ K⁻¹ at 873K for b. These values limit the families of n-type materials that could be associated to BaCu₂Se₂ in a thermoelectric module, as their respective coefficient of thermal expansion should match well.

As mentioned in the experimental section, Ba_{1-x}Na_xCu₂Se₂ powders and pellets were synthesized under vacuum during the entire synthesis process. Therefore, there could be some issues about the stability of these compounds in ambient conditions, as Na could easily react with CO₂ or water. Fig. 8 a) shows the XRD patterns of Ba_{0.9}Na_{0.1}Cu₂Se₂ powder stored during one month in ambient condition, and of Ba_{0.9}Na_{0.1}Cu₂Se₂ put in water during one week at room temperature, respectively. Surprisingly, both XRD patterns are the same as the corresponding freshly prepared sample (Fig. 1), which indicates that the Ba_{0.9}Na_{0.1}Cu₂Se₂ are air and water stable. However, the compounds rapidly degrade when heated at moderate temperature. As it can be observed in Fig. 8b), BaCu₂Se₂ powder starts to volatilize at a temperature as low as 473K, and rapidly almost completely volatilizes above 623K (the horizontal straight line on the TGA curve at a weight loss of about -63% corresponds to the saturation of the analyzer).

The inset of Fig. 8b) shows the TGA at 523K of a SPSed BaCu₂Se₂ pellet, with a density of 94% of the theoretical density. Even with almost full density and at a moderate temperature, the sample volatilizes, with a weight loss as large as 0.1% after only 2h at 523K. This volatilization would preclude the use of these materials in real modules used for waste heat conversion at high temperature. Therefore, it would be of great interest to find some coatings to limit the volatilization of the material, similarly to the coatings that have been developed for n-type skutterudites to limit the volatilization of antimony and make them usable in thermoelectric modules³⁹.

Conclusion

Na-doped BaCu₂Se₂ samples were prepared by solid-state reaction followed by spark plasma sintering densification. All samples were p-type with large Seebeck coefficient and very low thermal conductivity. The electrical conductivity can be strongly improved from 3.1 Scm⁻¹ for BaCu₂Se₂ to 440 Scm⁻¹ for Ba_{0.925}Na_{0.075}Cu₂Se₂ at 300 K due to the increased carrier concentration, leading to an enhanced power factor of 2.7 μWcm⁻¹K⁻² at 300K and 8.2μWcm⁻¹K⁻² at 773K. A ZT of 1.0 has been achieved at 773 K for doped BaCu₂Se₂, which is the highest values reported in the BaCu₂Ch₂ (Ch=S, Se and Te) family. However, the low evaporation temperature, hardly larger than 473K, limits its potential in thermoelectric modules at high temperature and would require the development of protective coatings to limit the materials degradation.

ACKNOWLEDGMENT

This work was supported by the ANR through the project OTHer (ANR 2011 JS08 012 01) and National Natural Science Foundation of China (No.51471061 and 51271069). This contribution was also supported by the Program for New Century Excellent Talents in University of Ministry of Education of China (NCET-12-0160).

REFERENCES

- ¹ K. Mitchell and J. A. Ibers, Chem. Rev., 2002, **102**, 1929.
- ² B. Kuropatwa, Y. Cui, A. Assoud and H. Kleinke, Chem. Mater., 2009, **21**, 88.
- ³ Y. Li, Q. Han, T. W. Kim and W. Shi, Nanoscale, 2014, **6**, 3777.
- ⁴ I. Ijjaali, K. Mitchell and J. A. Ibers, J. Solid State Chem., 2004, **177**, 760.
- ⁵ H. Yanagi, S. Ohno and T. Kamiy, J. Appl. Phys., 2006, **100**, 033717.
- ⁶ Y. S. Hor, A. J. Williams, J. G. Checkelsky, P. Roushan, J. Seo, Q. Xu, H.W. Zandbergen, A.

- Yazdani, N. P. Ong and R. J. Cava, *Phys. Rev. Lett.*, 2010, **104**, 057001.
- ⁷ W. C. Sheets, E. S. Stampler and H. Kabbour, *Inorg. Chem.*, 2007, **46**, 10741.
- ⁸ Li-Dong Zhao, Jiaqing He, David Berardan, Yuanhua Lin, Jing-Feng Li, Ce-Wen Nan and Nita Dragoe, *Energy Environ. Sci.*, 2014, **7**, 2900.
- ⁹ F. J. Fan, B. Yu, Y. X. Wang, Y. L. Zhu, X. J. Liu, S. H. Yu and Z. Ren, *J. Am. Chem. Soc.* 2011, **133**, 15910.
- ¹⁰ (a)M. Ibáñez, R. Zamani, A. LaLonde, D. Cadavid, W. Li, A. Shavel, J. Arbiol, J. R. Morante, S. Gorsse, G. J. Snyder and A. Cabot, *J. Am. Chem. Soc.*, 2012, **134**, 4060; (b) W. G. Zeier, A. LaLonde and Z. M. Gibbs, *J. Am. Chem. Soc.*, 2012, **134**, 7147; (c) W. G. Zeier, Y. Pei, G. Pomrehn, T. Day, N. Heinz, C. P. Heinrich, G. J. Snyder and W. Tremel, *J. Am. Chem. Soc.*, 2013, **135**, 726; (d)C. P. Heinrich, T. W. Day, W. G. Zeier, G. Snyder and W. Tremel, *J. Am. Chem. Soc.*, 2014, **136**, 442.
- ¹¹ (a)C. Sevik and T. Çağina, *Appl. Phys. Lett.*, 2009, **95**, 112105; (b)M. L. Liu, F. Q. Huang, L. D. Chen and I. W. Chen, *Appl. Phys. Lett.*, 2009, **94**, 02103; (c)F. J. Fan, Y. X. Wang, X. J. Liu, L. Wu and S. H. Yu, *Adv. Mater.*, 2012, **24**, 6158; (d)Y. Dong, H. Wang and S. George, *Inorg. Chem.* 2013, **52**, 14364.
- ¹² (a)E. J. Skoug, J. D. Cain and D. T. Morelli, *Appl. Phys. Lett.*, 2011, **98**, 261911; (b)D. Li, R. Li, X. Y. Qin, C. J. Song, H. X. Xin, L. Wang, J. Zhang, G. L. Guo, T. H. Zou, Y. F. Liu and X. G. Zhu, *Dalton Trans.*, 2014, **43**, 1888.
- ¹³ J. Fan, W. Carrillo-Cabrera, L. Akselrud, I. Antonyshyn, L. Chen and Y. Grin, *Inorg. Chem.*, 2013, **52**, 11067.
- ¹⁴ (a)S. Ishiwata, Y. Shiomi, J. S. Lee, M. S. Bahramy, T. Suzuki, M. Uchida, R. Arita, Y. Taguchi and Y. Tokura, *Nat. Mater.*, 2013, **12**, 512; (b)A.J. Hong, L. Li, H.X. Zhu, X.H. Zhou, Q.Y. He, W.S. Liu, Z.B. Yana, J. M. Liu and Z.F. Ren, *Solid State Ionics*, 2014, **261**, 21; (c) S. N. Guin, J. Pan, A. Bhowmik, D. Sanyal, U. V. Waghmare, and K. Biswas, *J. Am. Chem. Soc.*, 2014, **136**, 12712.
- ¹⁵ (a) H. Liu, X. Shi, F. Xu, L. Zhang, W. Zhang, L. Chen, Q. Li, C. Uher, T. Day and G. J. Snyder, *Nat. Mater.*, 2012, **11**, 422; (b) Y. He, T. Day, T. Zhang, H. Liu, X. Shi, L. Chen and G. J. Snyder, *Adv. Mater.*, 2014, **26**, 3974.
- ¹⁶ X. Lu , D. T. Morelli, Y. Xia, F. Zhou, V. Ozolins, H. Chi, X. Zhou, and C. Uher, *Adv. Energy Mater.*, 2013, **3**, 342.
- ¹⁷ R. Liu, L. Xi, H. Liu, X. Shi, W. Zhang and L. Chen, *Chem. Commun.*, 2012, **48**, 3818.
- ¹⁸ T. Plirdpring, K. Kurosaki, A. Kosuga, T. Day, S. Firdosy, V. Ravi, G. J. Snyder, A. Harnwungmoung, T. Sugahara, Y. Ohishi, H. Muta and S. Yamanaka, *Adv. Mater.*, 2012, **24**, 3622.
- ¹⁹ J. Huster and W. Z. Bronger, *Anorg. Allg. Chem.*, 1999, **625**, 2033.
- ²⁰ K. Kurosaki, H. Uneda, H. Muta and S. Yamanaka, *J. Appl. Phys.*, 2005, **97**, 053705.

- ²¹ M. A. McGuire, A. F. May, D. J. Singh, M. H. Du and G. E. Jellison, *J. Solid State Chem.*, 2011, **184**, 2744.
- ²² Y.C. Wang and F.J. DiSalvo, *J. Solid State Chem.*, 2001, **156**, 44.
- ²³ A. Assoud, Y. Cui, S. Thomas, B. Sutherland and H. Kleinke, *J. Solid State Chem.*, 2008, **181**, 2024.
- ²⁴ K. Kurosaki, H. Uneda, H. Muta and S. Yamanaka, *J. Alloy. Compd.*, 2004, **385**, 312.
- ²⁵ G.B. Liu, X.Q. Wang, X.J. Kuang and A. L. He, *Physica B*, 2010, **405**, 4582.
- ²⁶ A. Krishnapriyan, P. T. Barton, M. Miao and R. Seshadri, *J. Phys.: Condens. Matter.*, 2014, **26**, 155802.
- ²⁷ G. Rogl, A. Grytsiv, P. Rogl, E. Bauer, M.B. Kerber, M. Zehetbauer and S. Puchegger, *Intermetallics*, 2010, **18**, 2435.
- ²⁸ A.F. May, E. S. Toberer, A. Saramat and G.J. Snyder, *Phys. Rev. B*, 2009, **80**, 125205.
- ²⁹ M.G. Kanatzidis, S.D. Mahanti and T.P. Hogan (Eds.), *Chemistry, Physics, and Materials Science of Thermoelectric Materials*, Kluwer Academic/Plenum Publishers, New York, 2002.
- ³⁰ G.S. Nolas, J. Sharp and H.J. Goldsmid (Eds.), *Thermoelectrics—Basic Principles and Materials Development*, Springer Series in Materials Science, vol. 45, Springer, Berlin, 2001.
- ³¹ D.M. Rowe (Ed.), *CRC Handbook of Thermoelectrics*, CRC Press Inc., Boca Raton, FL, 1995.
- ³² D.M. Rowe (Ed.), *Thermoelectrics Handbook—Macro to Nano*, CRC Press Inc., FL, 2005.
- ³³ K. Biswas, J. He, Q. Zhang, G. Wang, C. Uher, V. P. Dravid and M. G. Kanatzidis, *Nat. Chem.*, 2011, **3**, 160.
- ³⁴ S. N. Girard, J. He, X. Zhou, D. Shoemaker, C. M. Jaworski, C. Uher, V. P. Dravid, J. P. Heremans and M. G. Kanatzidis, *J. Am. Chem. Soc.*, 2011, **133**, 16588.
- ³⁵ L. D. Zhao, H. J. Wu, S. Q. Hao, C. I. Wu, X. Y. Zhou, K. Biswas, J. Q. He, T. P. Hogan, C. Uher, C. Wolverton, V. P. Dravid and M. G. Kanatzidis, *Energy Environ. Sci.*, 2013, **6**, 3346.
- ³⁶ Y. Lee, S. H. Lo, J. Androulakis, C. I. Wu, L. D. Zhao, D. Y. Chung, T. P. Hogan, V. P. Dravid and M. G. Kanatzidis, *J. Am. Chem. Soc.*, 2013, **135**, 5152.
- ³⁷ W. S. Liu, Q. Zhang, Y. Lan, S. Chen, X. Yan, Q. Zhang, H. Wang, D. Wang, G. Chen and Z. Ren, *Adv. Energy Mater.*, 2011, **1**, 577.
- ³⁸ C. J. Liu, H. C. Lai, Y. L. Liu and L. R. Chen, *J. Mater. Chem.*, 2012, **22**, 4825.
- ³⁹ J.S. Sakamoto, T. Caillat, J.P. Fleurial, G.J. Snyder, United States Patent, No.: US 7,480,984 B1, Date of Patent: Jan., 2009, **27**.

Figure Caption

Fig. 1 a) X-ray diffraction pattern and Rietveld refinement of BaCu_2Se_2 powder; b) Crystal structure of BaCu_2Se_2 .

Fig. 2 a) XRD patterns; b) Lattice parameters of $\text{Ba}_{1-x}\text{Na}_x\text{Cu}_2\text{Se}_2$ samples; c) Diffuse reflectance of BaCu_2Se_2 .

Fig. 3 a) Scanning electron micrographs of $\text{Ba}_{0.9}\text{Na}_{0.1}\text{Cu}_2\text{Se}_2$; X-ray Element mapping images of b)Ba, c)Na, d)Cu, and e) Se in $\text{Ba}_{0.9}\text{Na}_{0.1}\text{Cu}_2\text{Se}_2$.

Fig. 4 a) Hall carriers concentration and mobility in $\text{Ba}_{1-x}\text{Na}_x\text{Cu}_2\text{Se}_2$ series (the solid line corresponds to the nominal carriers concentration estimated assuming one free hole per sodium atom); b) Temperature dependence of the holes mobility of $\text{Ba}_{0.98}\text{Na}_{0.02}\text{Cu}_2\text{Se}_2$.

Fig. 5 Thermoelectric properties as a function of temperature for $\text{Ba}_{1-x}\text{Na}_x\text{Cu}_2\text{Se}_2$ samples: a), b) Electrical conductivity; c), d) Seebeck coefficient and e), f) Power factor.

Fig. 6 Thermoelectric properties as a function of temperature for $\text{Ba}_{1-x}\text{Na}_x\text{Cu}_2\text{Se}_2$ samples: a) Specific heat; b) Thermal diffusivity; c) Total thermal conductivity; d) Lattice thermal conductivity; e) Electric thermal conductivity; and f) Figure of merit ZT.

Fig. 7 a) XRD patterns of BaCu_2Se_2 as a function of temperature; b) Temperature dependence of the lattice parameters.

Fig. 8 XRD patterns of $\text{Ba}_{0.9}\text{Na}_{0.1}\text{Cu}_2\text{Se}_2$ a) after one month storage in ambient conditions and after one week in water; b) Thermogravimetric analysis of BaCu_2Se_2 powder and densified pellet (inset).

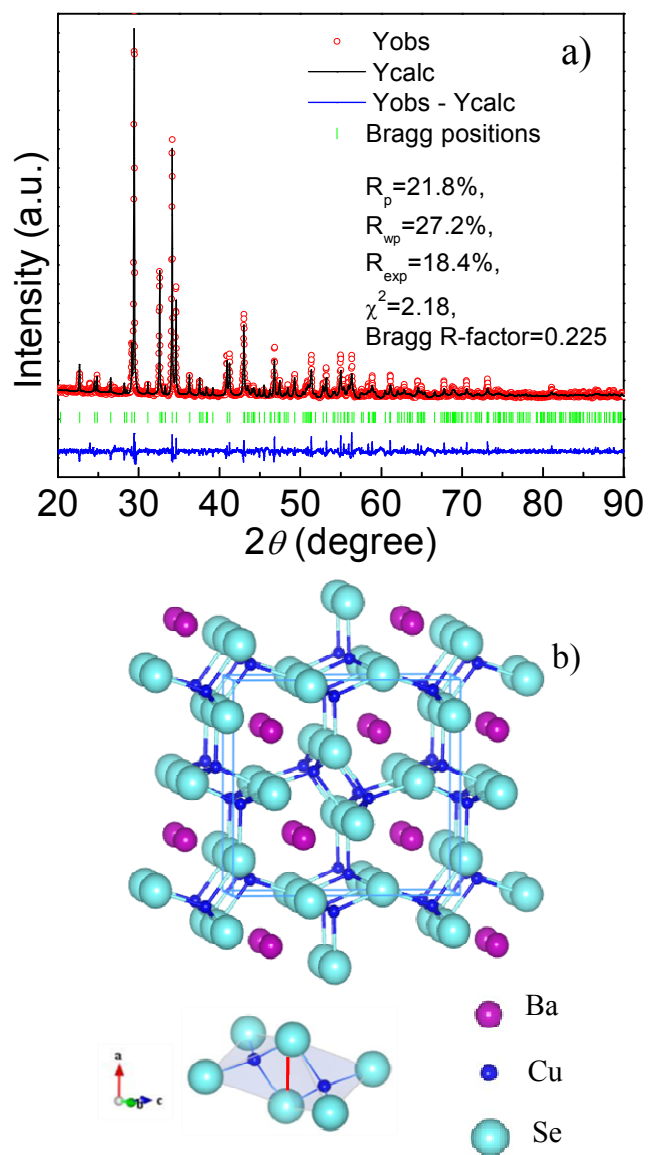


Fig. 1

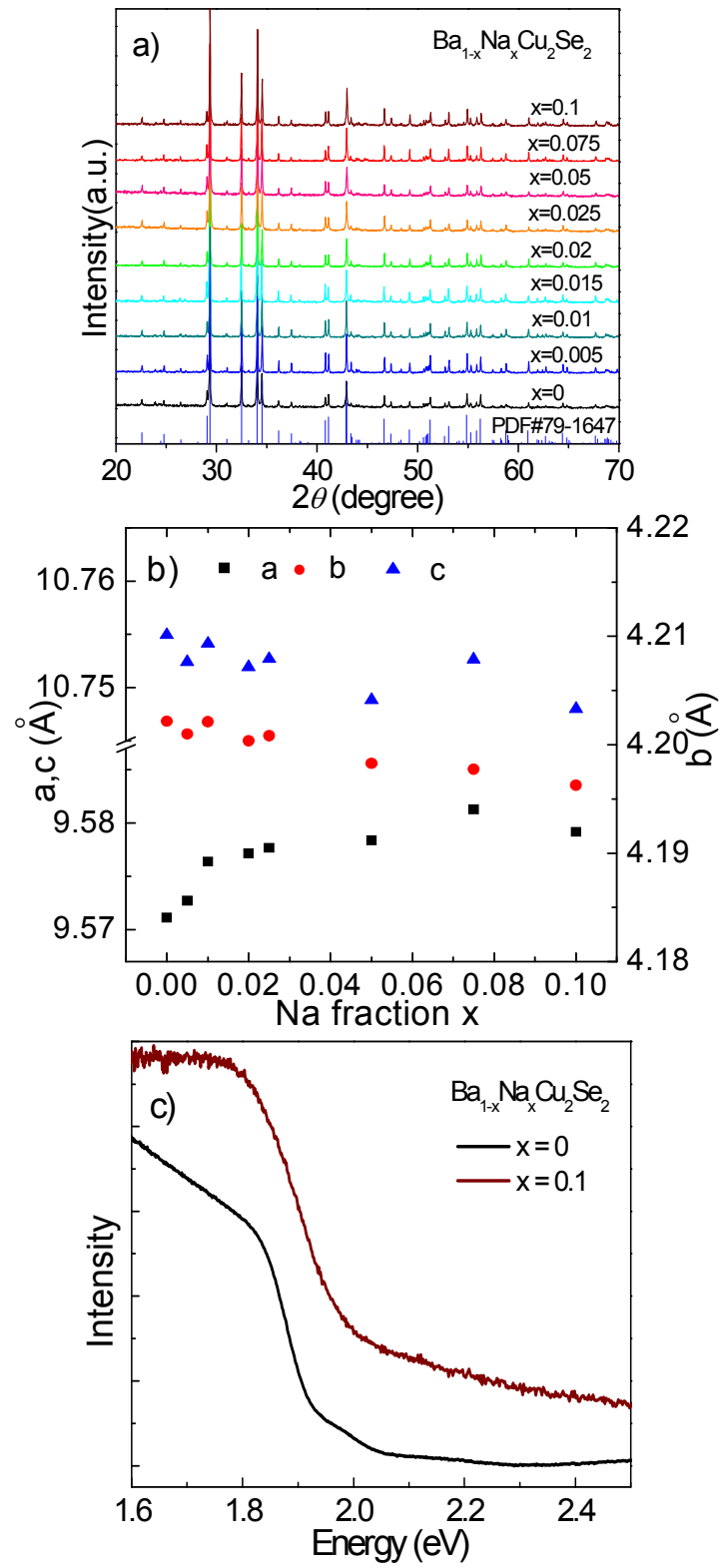


Fig. 2

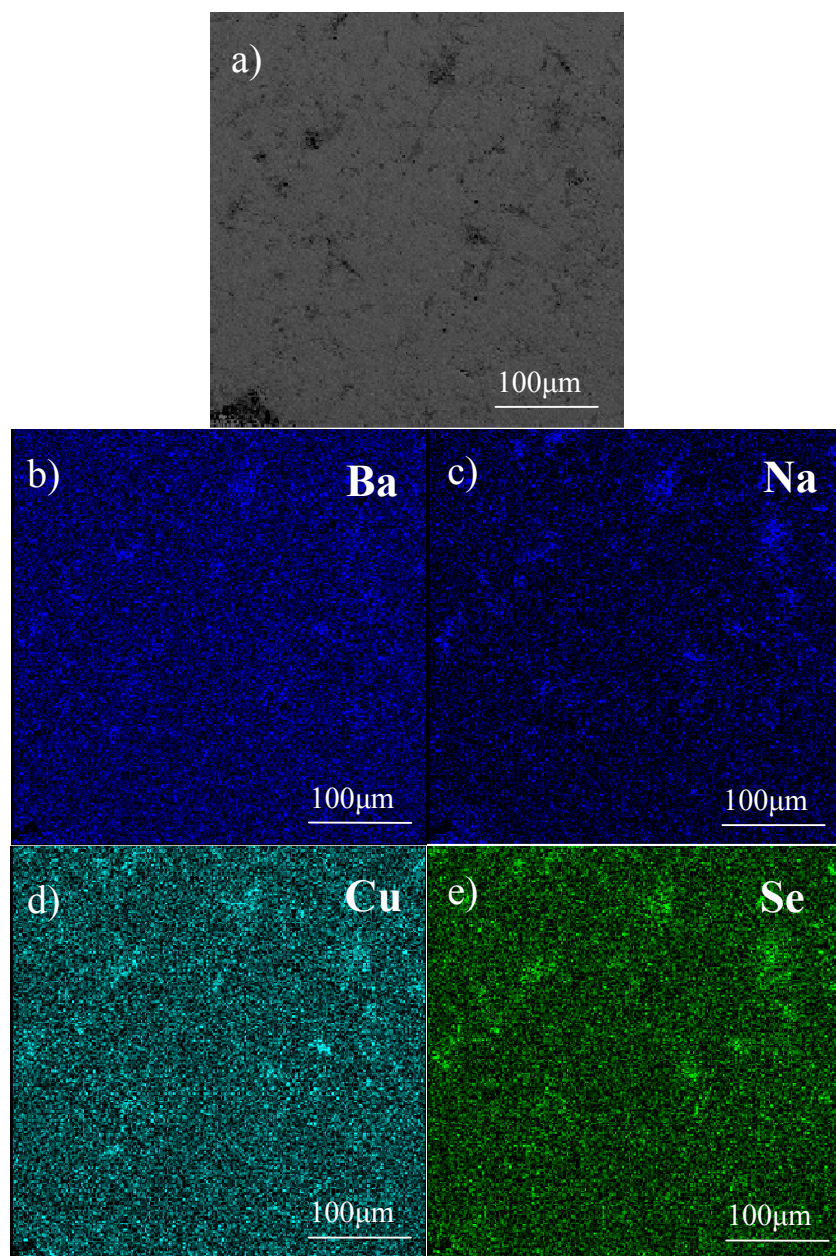


Fig. 3

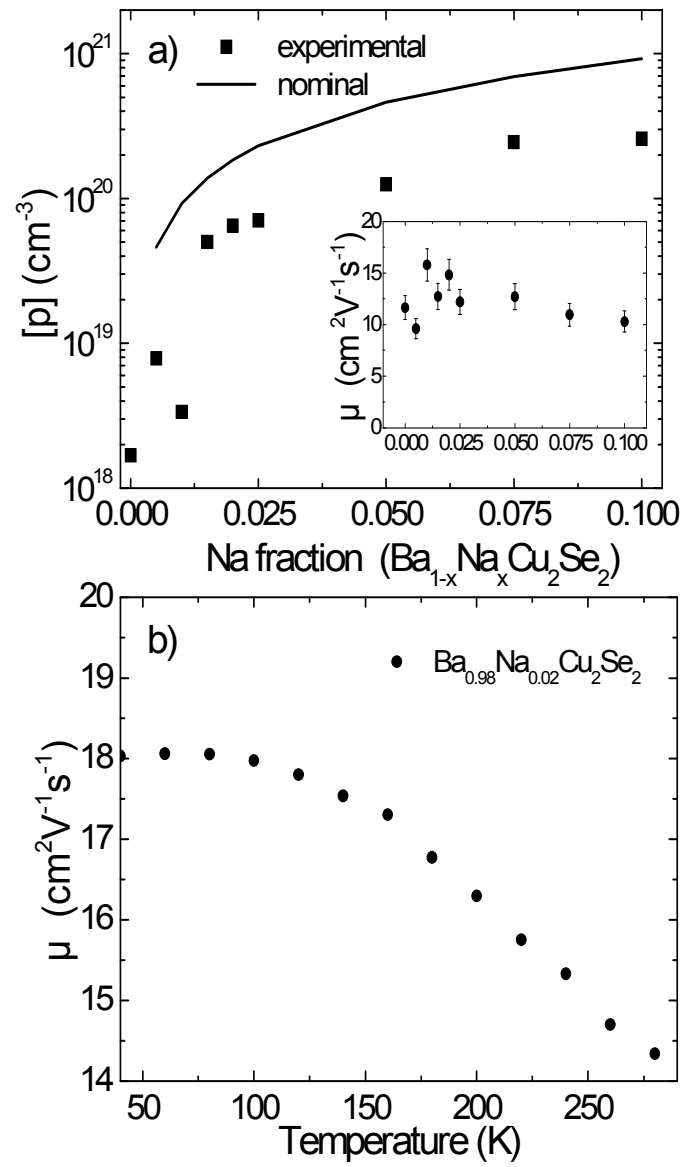


Fig. 4

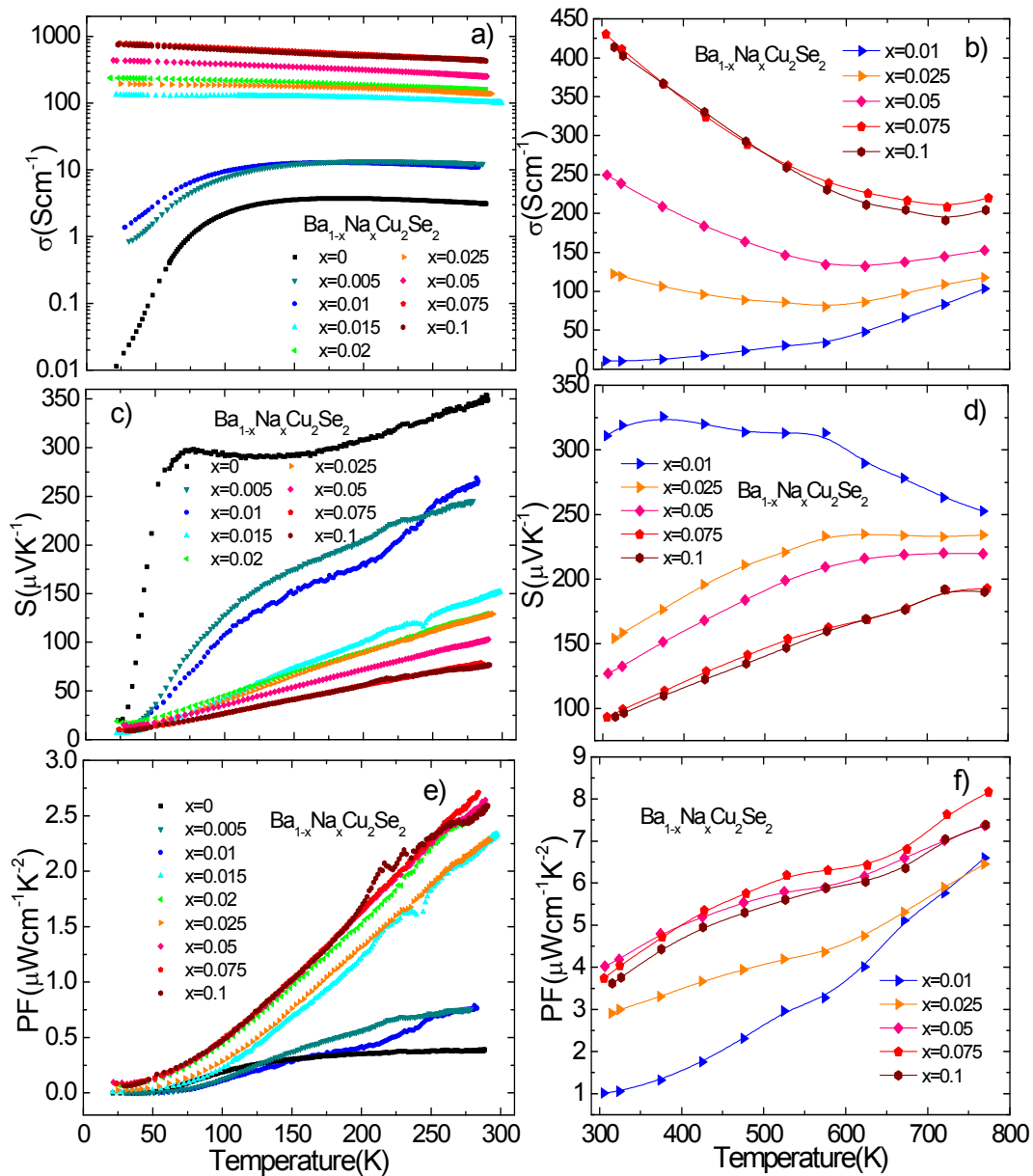


Fig. 5

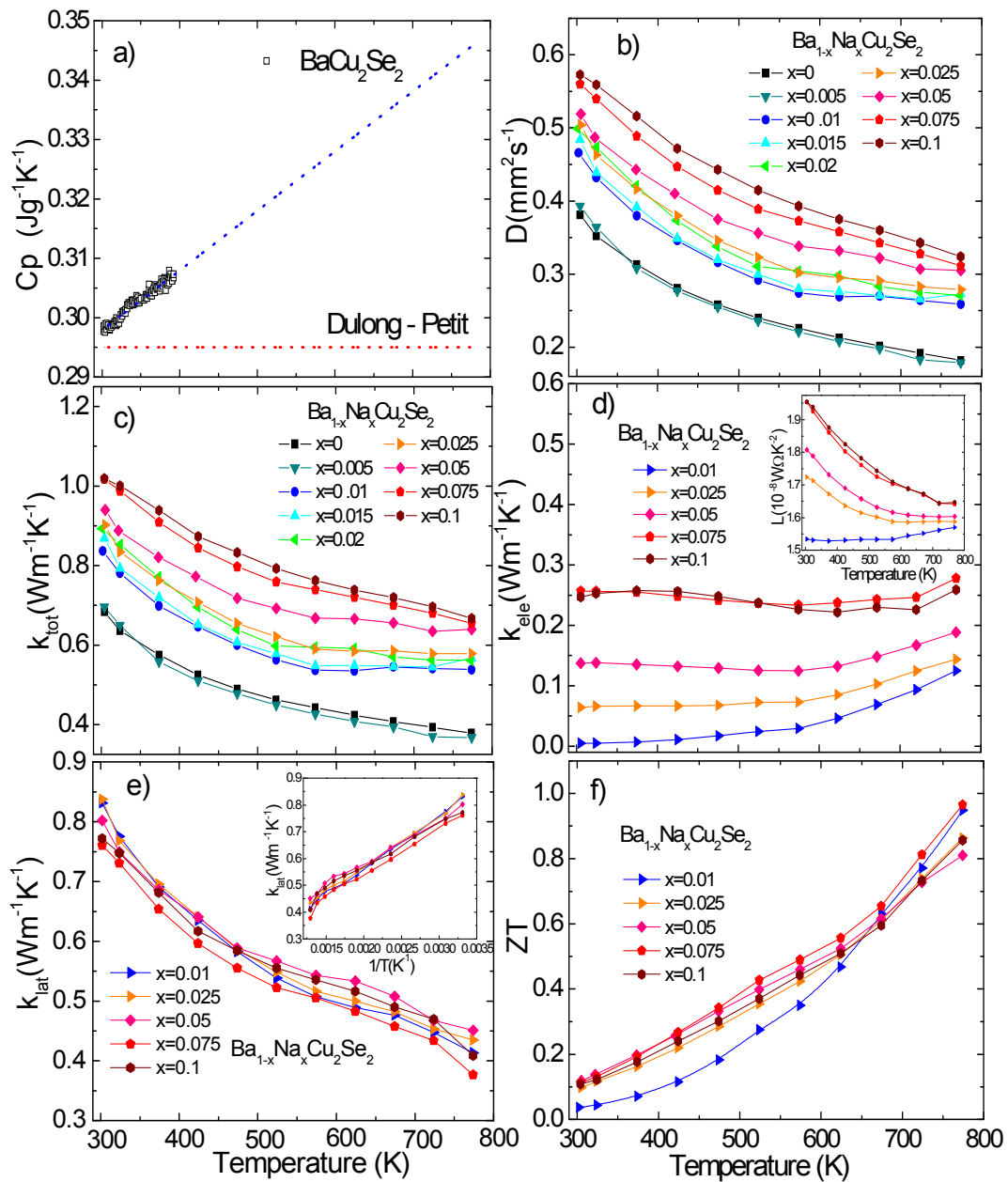


Fig. 6

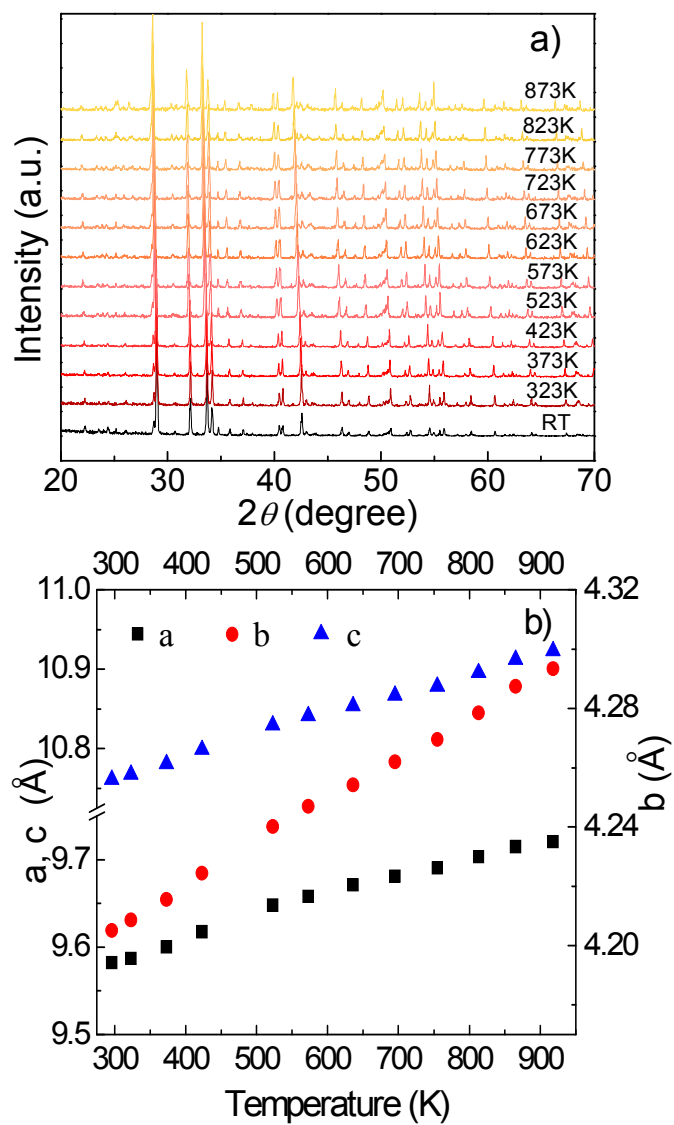


Fig. 7

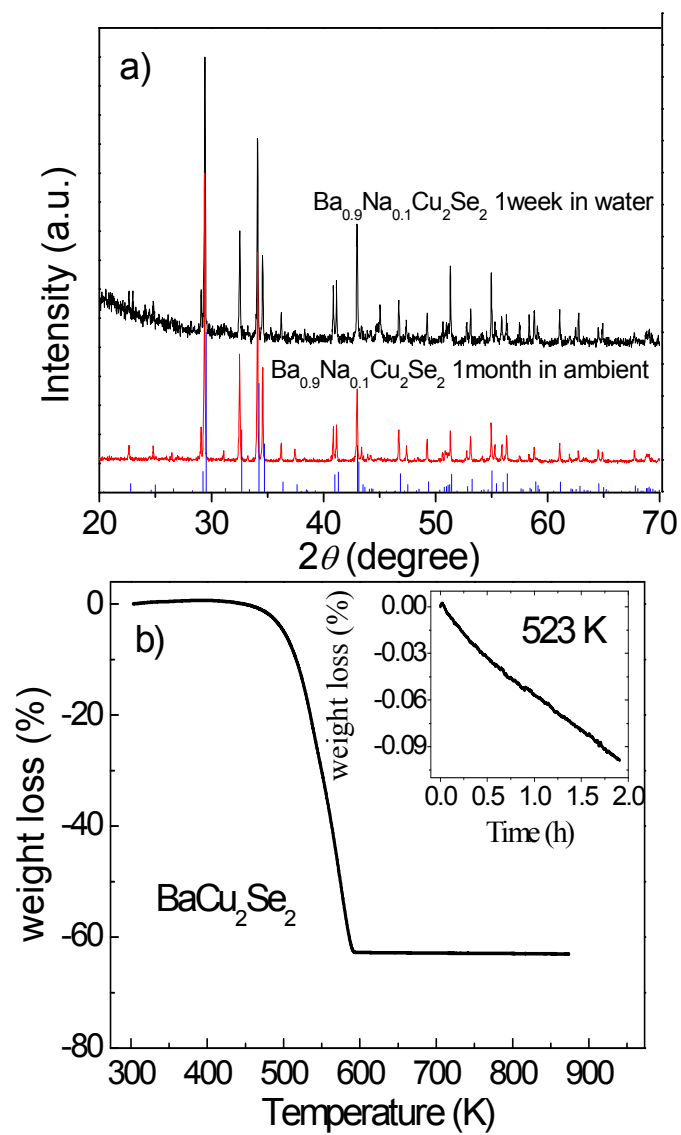


Fig. 8

Graphical Abstract

Thermoelectric properties of Na doped BaCu_2Se_2 was studied. The electric conductivity of BaCu_2Se_2 was increased by 2 orders of magnitude through Na doping at Ba sites, combined with a surprisingly low thermal conductivity, ZT of 1.0 has been obtained for $\text{Ba}_{0.925}\text{Na}_{0.075}\text{Cu}_2\text{Se}_2$ at 773K.

